J Therm Anal Calorim (2015) 122:975–984
DOI 10.1007/s10973-015-4801-z

Pyrolysis characteristics and kinetics of two Chinese low-rank coals

Ying Xu[1] · Yongfa Zhang[1] · Guojie Zhang[1] · Yunfei Guo[1] · Jing Zhang[1] · Guoqiang Li[1]

Received: 20 December 2014 / Accepted: 25 May 2015 / Published online: 20 June 2015

Abstract The pyrolysis characteristics and kinetics of two Chinese low-rank coal samples have been studied through thermogravimetric technique and mathematical modeling. Applicability of three kinetic models, viz. the Doyle temperature integral model, Achar–Brindley–Sharp–Wendworth (ABSW) derivative model and Coats–Redfern integral model, is evaluated. The results showed that Doyle model and ABSW model cannot describe the pyrolysis process accurately, while Coats–Redfern integral model was appropriate to describe pyrolysis reaction of the two low-rank coals. From the Coats–Redfern integral model, the reaction order of low-rank coals was of $n = 2$, and the pyrolysis process can be divided into four stages; the activation energy decreased with increasing heating rate above 20 K min^{-1} and increased continuously with the coalification degree.

Keywords Low-rank coal · Pyrolysis · Model · Kinetics · TG

Introduction

Low-rank coal deposit is about 55 % in the total reserves of coal in China [1], but the low-rank coal utilization is inefficient because of its high content of water, volatile matter and oxygen but low calorific value. As the pyrolysis is the first step in all thermochemical coal conversion processes, "key technologies and demonstration on clean and efficient utilization of low-rank coal," which was put forward by Chinese Academy of Sciences, aim to make some development in low-rank coal pyrolysis in the forerunner of the comprehensive utilization. Although much work has been conducted to study coal pyrolysis [2–4], few studies on pyrolysis mechanism of low-rank coal have been conducted. Therefore, it is necessary to establish the mechanism function and kinetic parameters of low-rank coals.

Thermogravimetric analysis (TG) is one of the most important techniques used to study thermal events. In order to evaluate the kinetic data and to establish reliable models for the complex reaction scheme of coal pyrolysis, TG data were studied which were depended on the temperature at defined heating rate or on the time at a constant temperature (static measurement) [5, 6]. Thus, thermal analysis kinetics is a useful way to study the physical change or chemical reaction during thermal process, such as judging the followed mechanism of reaction [reaction mechanism function, $f(\alpha)$] and obtaining kinetic rate parameters (the activation energy E and pre-exponential factor A) [7]. In early research on this complex problem, isothermal method models were used, but it has been shown that they are applicable only under limited conditions [8]. To simulate the kinetics of coal during its thermal decomposition, a more complex model is required, known as the non-isothermal method [9]. Non-isothermal method can be divided into derivative method and integral method according to the form of the kinetic equation [10]. Many works have focused on using single non-isothermal method kinetics model to study coal thermal decomposition [11–14], and there is still necessary to compare the two non-isothermal methods to decide which one is more adaptive for describing the pyrolysis of coal.

✉ Ying Xu
xuying@tyut.edu.cn

✉ Yongfa Zhang
yongfaz@tyut.edu.cn

[1] Key Laboratory of Coal Science and Technology, Ministry of Education and Shanxi Province, Taiyuan University of Technology, Taiyuan 030024, People's Republic of China

This paper aims to compare the kinetic parameters calculated for the pyrolysis of Chinese low-rank coals by using three non-isothermal experimental method including a derivative method and two integral methods, applying the same data treatment in both cases. In this way, the differences in results that can be attributed to the experimental technique will be determined. This aspect is very important because no comparison has been made before.

Experimental

Coal characteristics

The investigations were performed on two low-rank coals samples taken from the deposits in Yunnan Province (YN) and Xinjiang Province (XJ), China, respectively.

Proximate and ultimate analyses

The results of proximate and ultimate analyses of the two low-rank coals are given in Table 1. All the information reported in the table was provided by the State Key Laboratory of Coal Conversion, Shanxi Institute of Coal Chemistry, Chinese Academy of Sciences. For kinetic studies, the coal samples were dried at 110 °C for 2 h in an inert atmosphere of nitrogen, and then, the dried samples were further ground to a size of 90–150 micron.

The lignite YN presented higher content of volatile matter, higher content of oxygen and lower content of fixed carbon than those of XJ. Compared with the XJ coal, the higher H/C and O/C atomic ratios in the YN indicated the higher amount of aliphatic in the solid residues [15]. The H/C/O atomic ratio of YN was 0.98:1:0.42, while the number became to 0.59:1:0.21 in XJ indicating that the unsaturated bond number in the macromolecular structure of low-rank coal increased with increasing metamorphic degree of coal [16].

FTIR spectroscopy analysis

Fourier transform infrared (FTIR) spectra of the samples were recorded over the range of 4000–400 cm^{-1} on an American Bio-Rad FTS165 FTIR Spectrometer 1725X using the KBr pellet technique. The total numbers of scans were 32 with spectral resolution of 2 cm^{-1}. For the spectroscopic study (FTIR analysis), samples were prepared using the standard KBr pellet procedure for this type of material (lignite/KBr mixture at a 1:180 ratio). Figure 1 displays the FTIR spectra of the YN and XJ coals.

It can be seen that there was a significant absorption band at approximately $\sim$3490 cm^{-1}, which was assigned to OH groups. The absorption peaks of 3000–2700 cm^{-1} zone revealed three absorption peaks of the aromatic hydrogen, CH stretching and aliphatic hydrogen, and Figure 1 shows that the absorption peaks of YN were slightly more than those of XJ. A significant absorption peak for the oxygen-containing functional groups and C–O–R structures can also be observed in the 1800–1100 cm^{-1} zone and 1100 cm^{-1} zone, respectively. The higher absorption peaks of YN in the 1100 cm^{-1} than those of XJ mean that oxygen-containing functional groups number in coal decreased with increasing degree of coalification. The aromatic hydrogen was in 900–700 cm^{-1} zone [17]. Furthermore, the significant absorption band at approximately 1700 cm^{-1}, and the presence of structures containing C=O groups might be in agreement with the low rank of YN and XJ, which may also reveal that there was some resinite in the structures of these low-rank coals [18].

TG and DTG

A STA 409C Thermo-Gravimetric Analysis (TGA) apparatus was used to analyze the TG and DTG. About 10 mg of dried basis sample was used to experiment. The system was purged firstly with high-purity nitrogen, and then, the sample was heated up to 850 °C at a constant heating rate of 10, 20 and 30 °C min^{-1}, respectively. The carrier gas was N_2 with a flow rate of 60 mL min^{-1}.

Calculation of kinetic parameters

First, the two low-rank coals pyrolysis process was assumed as follows:

(a) High-purity nitrogen (99.999 %) was used as protective gas, and it had no influences to coal pyrolysis;
(b) It had no temperature gradient in coal sample interior during the pyrolysis heating process; in infinitesimal

Table 1 Proximate and ultimate analysis of coal samples

Sample	Proximate analysis/mass%				Ultimate analysis/mass% (dry basis)					Atomic ratio	
	Moisture (received basis)	Ash	Volatile (dry basis)	Fixed Carbon	C	H	O	N	S_t	H/C	O/C
YN	32.74	29.63	30.10	40.27	42.08	3.42	23.53	0.96	0.39	0.98	0.42
XJ	12.01	4.91	29.12	65.97	70.29	3.44	19.86	0.97	0.52	0.59	0.21

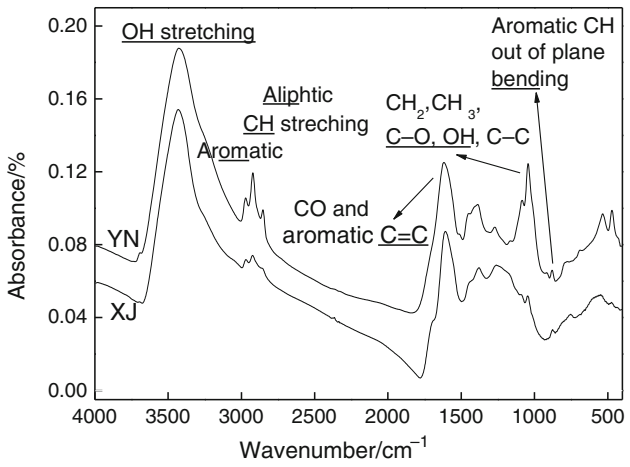

Fig. 1 FTIR spectra of the low-rank coals

time period, the pyrolysis non-isothermal method reaction can be seen as a isothermal method and heterogeneous reaction;

(c) Arrhenius expression was suitable for describing the two low-rank coals pyrolysis reaction:

$$\frac{d\alpha}{dt} = kf(\alpha) \tag{1}$$

where α is the pyrolysis conversion of initial material which derived from TG curves, t is the reaction time (min), $f(\alpha)$ is the function of unreacted initial sample and k is the rate constant, and k was typically correlated with temperature by an Arrhenius expression:

$$k = A\exp\left(-\frac{E}{RT}\right) \tag{2}$$

where A is the pre-exponential factor (min^{-1}), E is the apparent activation energy (kJ mol^{-1}), R is the gas constant (8.314 J mol^{-1} k^{-1}) and T is the absolute temperature (K).

The temperature dependency of the rate constant in Eq. (1) results in

$$\frac{d\alpha}{dT} = \frac{kf(\alpha)}{\beta} = \frac{A}{\beta}\exp\left(-\frac{E}{RT}\right)f(\alpha) \tag{3}$$

where A is the pre-exponential factor, E is the activation energy and β is the heating rate (dT/dt).

Results and discussion

Thermal behavior

To analyze the pyrolysis characteristics, the YN coal and XJ coal samples were pyrolyzed and analyzed with the TG system. The mass loss and mass loss rate curves under different heating rate are presented in Fig. 2.

Figure 2 shows that profiles of the TG and DTG curves of the two low-rank coals were being quite different.

The TG curves of the two low-rank coals decreased slowly at the temperature of 200–300 °C, and this was probably because of the softening and melting of coal at this temperature stage. The TG curves of YN coal were always higher than those of XJ under the same heating rate, and the result was consistent with the findings of some other study [19–21].

The DTG analysis showed that the slope of the DTG curve increased before the temperature of maximum rate of mass loss with the decreasing heating rate, which indicated that the decomposition process was a fast process; then DTG curve increased with increasing heating rate after the temperature of maximum rate of mass loss, indicating that the decomposition process was faster in higher temperature region.

The DTG curves went up to their maximum peak about the temperature of 450 °C, and the maximum peak value of YN lignite was greater than that of XJ coal; this was mainly due to the high hydrogen content of YN lignite, which means there was more aliphatic structure, aromatic alkyl

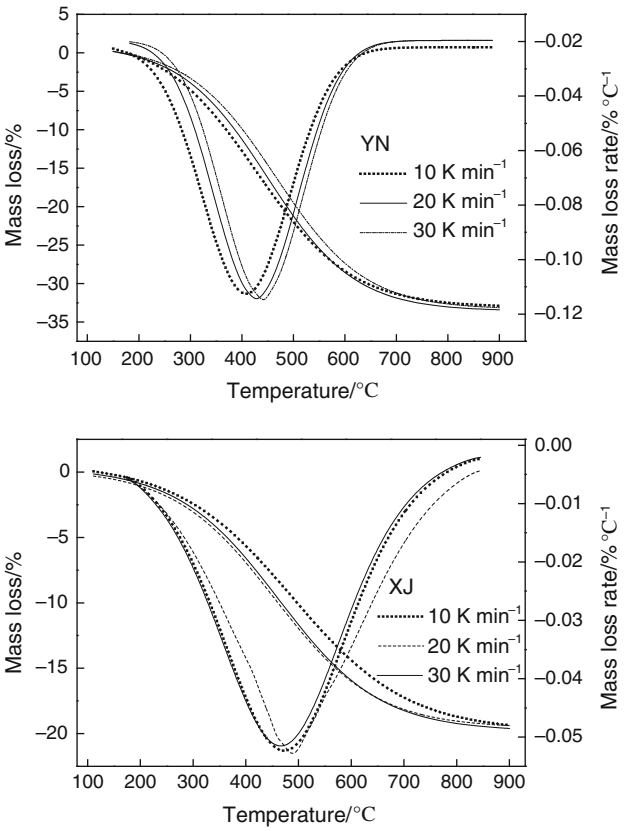

Fig. 2 TG and DTG curves of the two low-rank coals at different heating rate

side chain, the bridge bond and lower degree of condensation of aromatic hydrocarbon in lignite. When the coal was heated, some weak bonds such as aliphatic structure and bridge bond were cleaved into free radical fragments with large volumes of volatile matter releasing, and during this stage, it was the mainly depolymerization and decomposition with gas and tar precipitating, char formation [22, 23]. Then, TG curves and DTG curves decreased slightly with increasing temperature, and polycondensation became the main pyrolysis reaction. At this stage, the coal changed into char; meanwhile, methane and hydrogen were being the main composition of gas.

From Fig. 2, some characteristic parameters were obtained, including the following parameters: temperature of onset mass loss (T_{os}), temperature at the end of the reaction (T_f), the maximum mass loss rates (R_{max}) and the corresponding peak temperatures (T_{max}); the T_{os} is defined as temperature at $\alpha = 5\ \%$ and T_f is calculated at $\alpha = 85\ \%$. The thermogravimetric properties of the two low-rank coals are given in Table 2.

It can be seen that the total mass loss was increased with increasing coalification degree. The pyrolysis characteristic parameters such as T_{os}, T_f and T_{max} of XJ coal were about 15 °C higher than those of YN coal, which indicated that the pyrolysis was more difficult in high-rank coal with increasing thermal stability than that in lower-rank coal [24–26]. The R_{max} of YN coal presented higher values than that of XJ coal under the same heating rate, this may be related to large content of oxygen in lignite, and the oxygen-containing functional groups was easily broken because of its low bond energy.

For the same coal, the characteristic temperatures of T_{max} presented higher values with increasing heating rate. This effect indicates that the pyrolysis process may exist a temperature delay with the higher heating rate because it takes period of time to transmit heat quantity from surface to sample interior; there was not enough time for volatile releasing completely under high heating rate; the reaction temperature would move to a higher temperature too rapidly under high heating rate, but volatile matter could not release totally in such a short time.

Kinetics analysis

Doyle temperature integral model

Because of the complexity of coal pyrolysis, there are a variety of models to describe the pyrolysis process. Most researchers [27] described the coal pyrolysis by using the first-order reaction kinetic model, and kinetic parameters were obtained by using Doyle integral method. It is assumed that the decomposition rate of coal is equivalent to the volatizing rate [28], and the relationship between devolatilization rate and concentration was suitable for the Arrhenius expression equation of (3).

If $G(x) = kt$, when integrating both sides of Eq. (3) between $0 \sim \alpha$ and $T_0 \sim T$, respectively, Eq. (3) can be expressed as follows:

$$\int_0^{\alpha} \frac{\mathrm{d}\alpha}{f(\alpha)} = G(\alpha) = \frac{A}{\beta}\int_{T_0}^{T} \exp\left(-\frac{E}{RT}\right)\mathrm{d}T \tag{4}$$

Considering the reaction rate can be negligible under low temperature of T_0 at the beginning of reaction, the both sides of Eq. (4) can be integrated between $0 \sim \alpha$ and $0 \sim$ T as follows:

$$\int_0^{\alpha} \frac{\mathrm{d}\alpha}{f(\alpha)} = G(\alpha) = \frac{A}{\beta}\int_{0}^{T} \exp\left(-\frac{E}{RT}\right)\mathrm{d}T \tag{5}$$

In order to obtain the approximate solution of the temperature integral, just assumed that $u = \frac{E}{RT}$, then $T = \frac{E}{Ru}$ and

$$\mathrm{d}T = -\frac{E}{Ru^2}\mathrm{d}u \tag{6}$$

Then, Eq. (5) can be converted into equation as follows:

$$\begin{aligned} G(\alpha) &= \frac{A}{\beta}\int_0^{T} \exp\left(-\frac{E}{RT}\right)\mathrm{d}T = \frac{AE}{\beta R}\int_{\infty}^{u} \frac{-e^{-\mathrm{u}}}{u^2}\mathrm{d}u \\ &= \frac{AE}{\beta R}\int_{\frac{E}{RT}}^{+\infty} \frac{e^{-\mathrm{u}}}{u^2}\mathrm{d}u = \frac{AE}{\beta R}\cdot P(u) \end{aligned} \tag{7}$$

Table 2 Thermogravimetric properties of YN and XJ coals

Sample	Heating rate/°C min^{-1}	T_i/°C	T_{max}/°C	T_f/°C	R_{max}/% °C^{-1}
YN	10	213.3	453.9	633.2	0.107
	20	222.5	466.0	643.0	0.118
	30	243.7	472.6	668.1	0.120
XJ	10	227.5	471.0	677.0	0.075
	20	236.7	483.1	686.8	0.082
	30	257.9	489.8	711.4	0.084

where E/R is a constant, temperature integral of Eq. (7) is just become the problem of finding the function of $P(u) = \int_{\infty}^{u} \frac{-e^{u}}{u^2} \mathrm{d}u$; subsection integrated the above equation:

$$P(u) = \int_{\infty}^{u} \frac{-e^{u}}{u^2} \mathrm{d}u = \int_{\infty}^{u} \frac{1}{u^2} \mathrm{d}e^{-u} = \frac{e^{-u}}{u^2}\left(1 - \frac{2!}{u} + \frac{3!}{u^2} - \frac{4!}{u^3} + \cdots\right) \quad (8)$$

Then, it can be used Doyle model to approximately calculating Eq. (8). Calculating the logarithm of the first two items in parentheses:

$$\ln P(u) = -u + \ln(u-2) - 3\ln u \quad (9)$$

Because the range of u is $20 \le u \le 60$,

$$-1 \le \frac{u-40}{20} \le 1 \quad (10)$$

Assuming $v = \frac{u-40}{20}$ and then

$$u = 20v + 40 \quad (11)$$

Substituting Eq. (11) into Eq. (9) and deriving the first-order approximation for the logarithmic expansion terms:

$$\ln P(u) = -u - 3\ln 40 + \ln 38 + \ln\left(1 + \frac{10}{19}v\right) - 3\ln\left(1 + \frac{1}{2}v\right) \approx -5.3308 - 1.0516u \quad (12)$$

Assuming the pyrolysis is an first-order reaction, integrating the above equation with Eq. (3) and $\int_{0}^{\infty} \frac{\mathrm{d}\alpha}{(1-\alpha)} = -\ln(1-\alpha)$, then

$$\ln(-\ln(1-\alpha)) = \ln\left(\frac{AE}{\beta R}\right) - 5.384 - 0.1278\frac{E}{T} \quad (13)$$

Making linear regression to the plot of $\ln(-\ln(1-\alpha))$ versus $1/T$, $-E/R$ can be determined from the slope, A from the intercept. The pyrolysis kinetics parameters of YN and XJ coals at different heating rates are given in Table 3.

It can be seen from Table 3 that due to Doyle model, the pyrolysis process can be divided into four stages; the activation energy of each stage of XJ is larger than that of YN, which indicates that the activation energy is increased with the degree of coalification; for the same coal, the activation energy is decreased with increasing heating rate. The activation energy of first stage was the lowest; activation energy of second stage was increased rapidly, indicating that the phase was the active pyrolysis stage, the activation energy decreased slightly at the third stage, while the activation energy was the largest at the fourth stage.

Although some meaningful conclusions are obtained from Doyle model on describing pyrolysis of YN and XJ coals, the correlation coefficient of the dynamics curve is poor during the calculating of activation energy, which means it is not quite suitable to using Doyle model to describe the pyrolysis of the two low-rank coals.

Achar–Brindley–Sharp–Wendworth (ABSW) derivative model

According to ABSW derivative model [8], it needs to separate variables for Eq. (3) and calculate the logarithm on both sides, and then, Eq. (3) can be converted as follows:

$$\ln\left[\frac{\mathrm{d}\alpha}{f(\alpha)\mathrm{d}T}\right] = \ln\frac{A}{\beta} - \frac{E}{RT} \quad \left(\frac{\mathrm{d}\alpha}{\mathrm{d}t} = \beta\frac{\mathrm{d}\alpha}{\mathrm{d}T}\right) \quad (14)$$

Combining with $\mathrm{d}T = \beta \mathrm{d}t$, Eq. (2) can be converted as follows:

$$\ln\left[\frac{\mathrm{d}\alpha}{f(\alpha)\mathrm{d}T}\right] = \ln A - \frac{E}{RT} \quad (15)$$

If the pyrolysis reaction order is of $n = 1$ and $f(\alpha) = 1 - \alpha$, assuming that the pyrolysis process can be described by the single-reaction model of ABSW differential model, and the reaction order is of $n = 1$, and then plotting $\ln\left[\frac{\mathrm{d}\alpha/\mathrm{d}T}{1-\alpha}\right]$ versus $\frac{1}{T}$, using the least square method to fit the experimental data, where E can be determined from the slope of straight line A from the intercept simultaneously.

Because the drift of pyrolysis data under different heating rates is basically the same, Fig. 3 shows the relationship curve of $\ln\left[\frac{\mathrm{d}\alpha/\mathrm{d}T}{1-\alpha}\right]$ versus $\frac{1}{T}$ at heating rate of 10 K min^{-1} only.

Figure 3 shows that when the temperature is within a certain range of 724–833 K, the slope of the curve is positive, which means the corresponding activation energy of pyrolysis reaction is negative. The same thing has been happened on the pyrolysis data of other heating rate such as 20 and 30 K min^{-1}. So, the single-reaction model of ABSW derivative model cannot able to describe the pyrolysis process reasonably and give some theoretical explanation. The result was consistent with other research conclusion with some of other study [29].

Coats–Redfern integral model [30]

Calculation of kinetic parameters The pre-exponential factor, A, is assumed to be constant and independent of

Table 3 Kinetics of low-rank coals pyrolysis at different heating rates

	Heating rate/°C min^{-1}	Temperature/°C	Activation energy/kJ mol^{-1}	Pre-exponential factor/min^{-1}	R^2
YN	10	300–350	76.9	5.30×10^7	0.959
		350–500	101.01	1.37×10^3	0.952
		500–710	278.9	0.17×10^2	0.947
		710–850	103.7	0.52×10^3	0.934
	20	300–350	78.8	2.94×10^9	0.909
		350–500	100.1	8.67×10^3	0.936
		500–660	71.8	0.59×10^2	0.915
		660–850	102.6	1.60×10^3	0.929
	30	300–350	78.4	2.94×10^{10}	0.949
		350–520	99.6	1.42×10^4	0.952
		520–660	71.8	0.83×10^2	0.947
		660–850	105.5	2.95×10^3	0.901
XJ	10	300–390	100.3	2.13×10^9	0.944
		390–490	129.9	1.58×10^6	0.953
		490–710	108.6	4.16×10^4	0.957
		710–850	243.5	1.06×10^4	0.931
	20	300–400	83.7	1.63×10^9	0.912
		400–490	118.7	7.98×10^4	0.925
		490–700	100.0	0.77×10^3	0.908
		700–850	164.4	4.54×10^5	0.919
	30	300–410	73.9	2.61×10^9	0.934
		410–510	117.2	8.36×10^4	0.9867
		510–700	101.1	2.13×10^3	0.950
		700–850	162.8	4.33×10^5	0.889

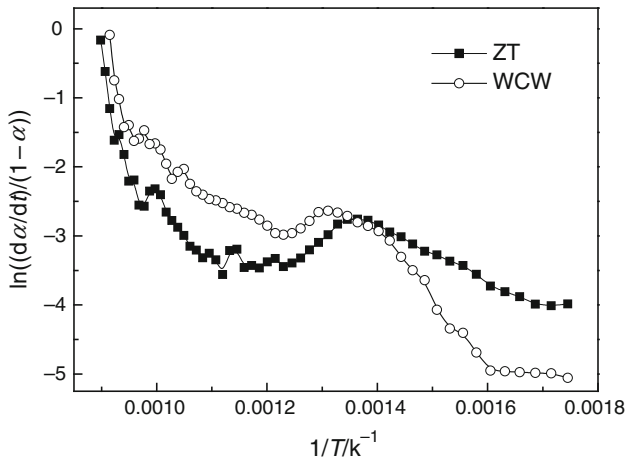

Fig. 3 Kinetic curves derived from ABSW model at heating rate of 10 K min^{-1}

temperature in this model, and this approach is advantageous and can be easily applied to study the kinetics of a temperature-programmed pyrolysis [31].

If the mass of sample was changed from w_0 (g) to w_t (g) with the reaction time t, then Eq. (2) can be expressed as follows:

$$\alpha = \frac{w_0 - w_t}{w_0 - w_\infty} = \frac{\Delta w}{\Delta w_f} \tag{16}$$

where W_0, W_t and W_∞ are the original mass (g) of the test sample, the mass (g) at time t or T and the final mass (g) at the end of pyrolysis, respectively.

If the sample is heated at a constant heating rate $\beta = \frac{dT}{dt}$, then Eq. (2) can be expressed as follows:

$$\frac{d\alpha}{dT} = \frac{kf(\alpha)}{\beta} = \frac{A}{\beta}\exp\left(-\frac{E}{RT}\right)f(\alpha) \tag{17}$$

Integrating Eq. (17):

$$\int_0^\alpha \frac{d\alpha}{f(\alpha)} = \frac{A}{\beta}\int_{T_0}^{T} \exp\left(-\frac{E}{RT}\right)dT \approx \frac{A}{\beta}\int_0^T \exp\left(-\frac{E}{RT}\right)dT \tag{18}$$

According to Coats–Redfern integral model, it can be assumed that two Chinese low-rank coals pyrolysis reaction followed the nth-order reaction:

$$y = (1-x)^n$$

$$n = 1, \quad f(\alpha) = 1 - \alpha,$$

$$\ln\left[\frac{-\ln(1-\alpha)}{T^2}\right] = \ln\left[\frac{AR}{\beta E}\left(1 - \frac{2RT}{E}\right)\right] - \frac{E}{RT} \tag{19}$$

$$n \neq 1, \quad f(\alpha) = (1-\alpha)^{n},$$
$$\ln\left[\frac{1-(1-\alpha)^{1-n}}{T^2(1-n)}\right] = \ln\left[\frac{AR}{\beta E}\left(1-\frac{2RT}{E}\right)\right] - \frac{E}{RT} \quad (20)$$

when $\frac{E}{RT} \gg 1$, $\left(1-\frac{2RT}{E}\right) \approx 1$, the first term of the right side in Eqs. (19) and (20) was almost a constant, and then the plot of $\ln\left[\frac{d\alpha/dT}{f(\alpha)}\right]$ versus $\frac{1}{T}$ gives a straight line, where E can be determined from the slope, while A can be determined from the intercept, and the YN and XJ pyrolysis reaction may be obtained with reaction order of n. Thus, n can be checked by a linear correlation and the E and A can be acquired simultaneously.

Based on the above-mentioned method of "calculation of kinetic parameters" at different heating rates of 10, 20 and 30 K min^{-1}, curves between $\ln\left[\frac{-\ln(1-\alpha)}{T^2}\right]$ $(n = 1)$, $\ln\left[\frac{1-(1-\alpha)^{1-n}}{T^2(1-n)}\right]$ $(n \neq 1)$ versus $\frac{1}{T}$ were concluded and are shown in Fig. 4 at different orders of $n = 1$, $n = 2$ and $n = 3$, respectively.

Figure 4 shows that the kinetic curves had four different ranges, and this was probably in accord with four different stages of the continuous chemical reaction in the lignite pyrolysis process. The kinetic curves gave a better correlation with the reaction orders of $n = 2$ than of $n = 1$ and $n = 3$; the heating rate had important influence on the kinetic curves probably because it can change the thermochemical reaction route and reaction mechanism in a degree.

The activation energy (E) and pre-exponential factor (A) were calculated and are given in Table 4 with reaction order of $n = 2$.

Table 4 shows that the activation energy of YN and XJ coals increased with increasing heating rate and then the activation energy decreased with increasing heating rate when it became above 20 K min^{-1}, and this result is just consistent with Chen's study [32]. The temperature of each pyrolysis stage also increased with increasing heating rate. The activation energy of low temperature decreased with increasing heating rate, while it just has a contrary changing trend with the heating rate during high-temperature period. The result of pyrolysis kinetics parameters at different heating rates can just indicate that there is some thermal hysteresis phenomenon during the pyrolysis at high heating rate [24, 25].

The activation energy of XJ coal was always higher than that of YN; this indicates that pyrolysis reaction process (mechanism) was quite different with coals themselves. That means there is a striking difference of molecular structure between coals which have different coal rank. In fact, the pyrolysis of coal is fundamentally a process of rupturing old bond and forming new bond, so the reaction process can partly reflect some characteristics of coal structure [33].

Table 4 shows that the pyrolysis process of the two low-rank coals can be divided into four stages. The activation energy of first stage of was the lowest, while that of second stage was increased rapidly, indicating that the phase was the active pyrolysis stage, the activation energy decreased slightly at the third stage, while the activation energy was the largest at the fourth stage.

In the first stage, the activation energy is relatively lower because it is just a releasing process of some gases with small molecules or some light molecules coming from rupturing of some weak bond.

In the second stage, the activation energy increases dramatically. Accompanied by the development of molecular bond breaking and hydrogen bond formation, a mass of macromolecular substance (such as tar and hydrocarbons) released [33]. The reactions of coal pyrolysis, depolymerization, formation of colloid and semi-char are occurred either in sequence or simultaneously which probably needs more energy, so the activation energy is larger than that of the first stage.

With the change in semi-char to char during the temperature of 500–600 °C, the physical framework of coal such as density, reflectance, diffraction peak intensity of characteristic X-ray diffraction and aromatic nucleus size increased slightly. But these indexes increased obviously at about 700 °C and then increased continuously with increasing temperature, which indicates that the degree of polycondensation reaction was enhanced rapidly [16]. This may be the reason why the activation energy increases dramatically during the temperature of 700–850 °C. Some people [34, 35] think that this is because of the low-rank coal's weak structure and poor thermal stability; it is still need to provide high energy for the releasing of massive volatile matter when the temperature is above 700 °C.

Verification of kinetic model In order to verify the accuracy of the kinetic model, the predictions using Coats–Redfern integral model for YN and XJ coals are compared with the experimental fractions.

Taking the second stage of pyrolysis and heating rate is of 20 K min^{-1} for an example, the temperature ranges of YN and XJ coals are 350–500 and 420–570 °C, respectively. Substituting the activation energy and the pre-exponential factor from Coats–Redfern integral model into Arrhenius Eq. (2):

$$k = A\exp\left(-\frac{E}{RT}\right) \quad (21)$$

Due to Coats–Redfern integral model, when $n = 2$,

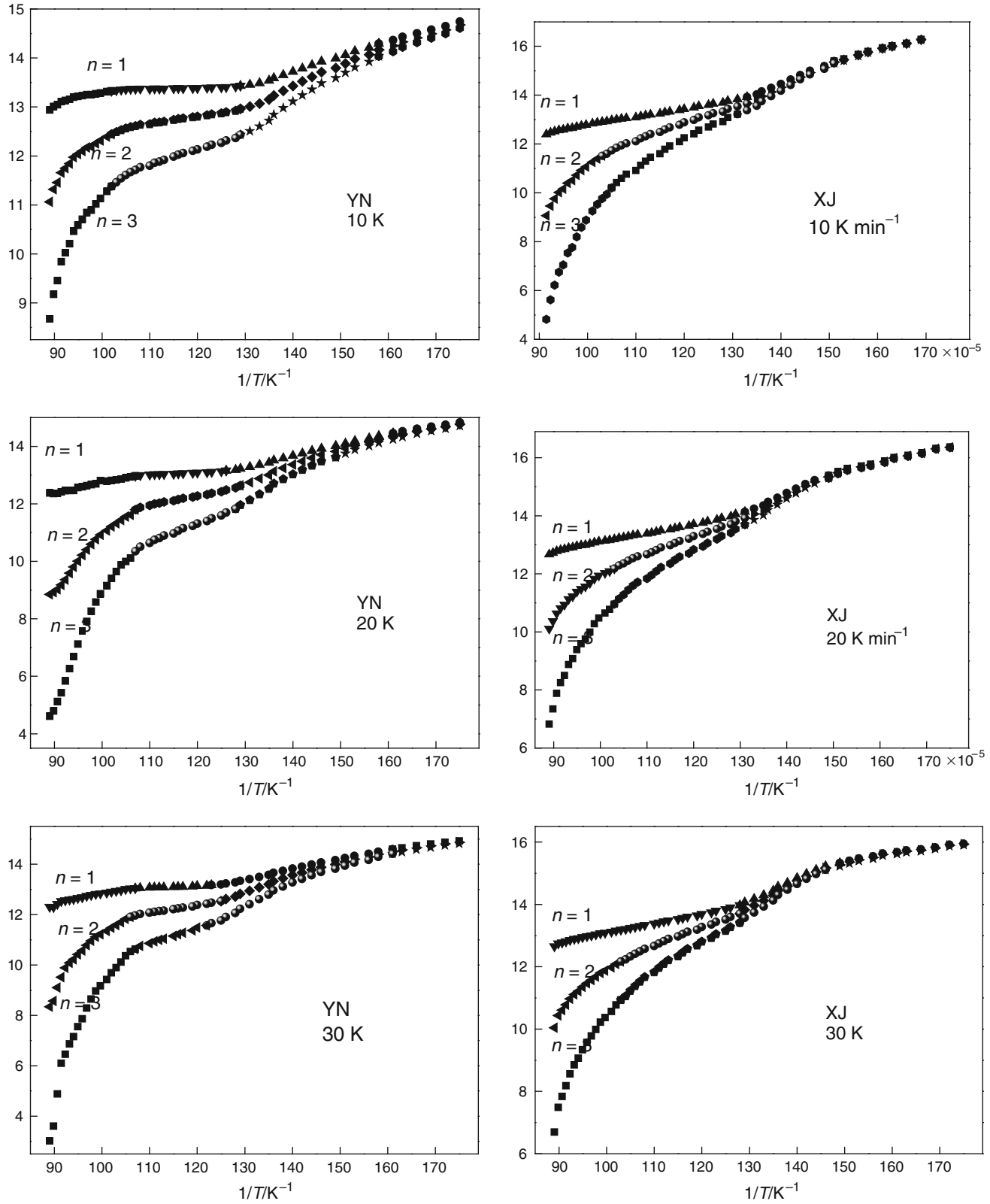

Fig. 4 Kinetic curves of the two low-rank coals derived from Coats–Redfern model at different heating rates

Table 4 Pyrolysis kinetics parameters of YN and XJ coals at different heating rates

	Heating rate/°C min^{-1}	Temperature/°C	Activation energy/kJ mol^{-1}	Pre-exponential factor/min^{-1}	R^2
YN	10	300–350	75.2	2.56	0.999
		350–500	96.3	0.29×10^2	0.998
		500–710	73.9	0.34	0.980
		710–850	130.9	6.74×10^3	0.912
	20	300–350	78.1	9.33	0.992
		350–500	99.2	7.82×10^2	0.995
		500–660	78.4	0.19×10^2	0.993
		660–850	197.1	9.63×10^3	0.966
	30	300–350	77.3	9.94	0.985
		350–550	101.0	1.34×10^3	0.995
		550–660	76.2	0.17×10^2	0.993
		660–850	213.4	2.42×10^4	0.904
XJ	10	320–390	99.4	1.03×10^2	0.975
		390–490	128.9	3.39×10^4	0.999
		490–700	108.3	8.53×10^2	0.993
		700–850	146.5	1.38×10^5	0.925
	20	300–400	82.3	5.16	0.993
		400–490	118.4	7.24×10^3	0.999
		490–700	99.3	2.51×10^2	0.998
		700–850	218.3	2.73×10^6	0.959
	30	300–410	71.8	0.88	0.975
		410–510	117.0	7.91×10^3	0.997
		510–700	100.3	4.45×10^2	0.995
		700–850	227.0	3.55×10^6	0.954

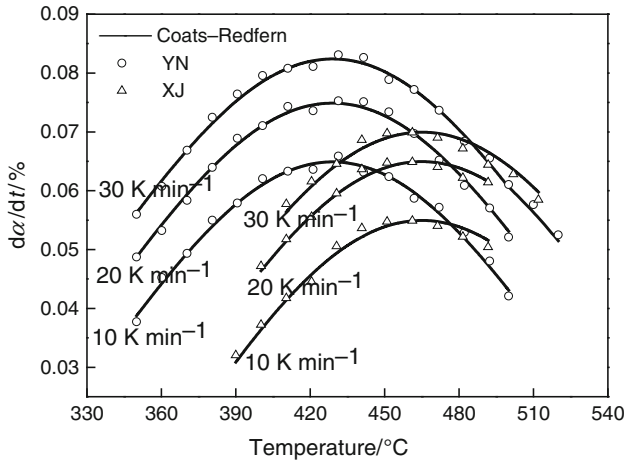

Fig. 5 Comparison of Coats–Redfern model predictions with experimental values of mass loss at the heating rate of 20 K min^{-1}

$$f(\alpha) = (1-\alpha)^2 \tag{22}$$

Substituting Eqs. (21) and (22) into Eq. (1) is solved for dα/dt.

The predictions using Coats–Redfern integral model for YN and XJ coals are compared with the experimental fractions of the second pyrolysis stage as shown in Fig. 5.

Figure 5 shows that the predictions of Coats–Redfern model are almost similar to the experimental fractions, which indicates that the model is able to explain the results satisfactorily.

Conclusions

Major conclusions from the test results can be summarized as follows:

(1) Doyle temperature integral model cannot describe the pyrolysis of the two Chinese low-rank coals accurately because of its poor correlation coefficient of the activation energy dynamics curve.

(2) The single-reaction model of ABSW derivative model was not able to describe the pyrolysis process reasonably and give some theoretical explanation for the negative activation energy during the temperature range of 724–833 K.

(3) The Coats–Redfern integral model was suitable to describe the pyrolysis process. Coats–Redfern integral model determined that the reaction order of low-rank coals was of $n = 2$ and the pyrolysis process

can be divided into four stages, while the activation energy of second stage was increased rapidly, indicating that the phase was the active pyrolysis stage in the low-temperature period.

(4) The pyrolysis activation energy of the two low-rank coals decreased with increasing heating rate above 20 K min^{-1}, while the activation energy always increased with the coalification degree.

Acknowledgements The project was supported by the National Science and Technology Pillar Program (Grant No. 2012BAA04B03), Natural Science Foundation of China (Grant Nos. 51274147 and 21376003), Program for the Outstanding Innovative Teams of Higher Learning Institutions of Shanxi and Shanxi Provincial Natural Science Foundation (Grant No. 2011021009-2).

References

1. Xu Y, Zhang GJ, Chen L. Pyrolysis products properties from lignite. Asian J Chem. 2013;25:4828–32.
2. Lei M, Wang C, Wang SJ. Effect of pyrolysis characteristics on ignition mechanism and NO emission of pulverized coal during oxy-fuel combustion. J Therm Anal Calorim. 2014;117:665–73.
3. Wang J, Yan Q, Zhao J, Wang ZQ. Fast co-pyrolysis of coal and biomass in a fluidized-bed reactor. J Therm Anal Calorim. 2014;118:1663–73.
4. Herce C, Caprariis B, Stendardo S. Comparison of global models of sub-bituminous coal devolatilization by means of thermogravimetric analysis. J Therm Anal Calorim. 2014;117:506–16.
5. Wu D, Liu G, Chen S. An experimental investigation on heating rate effect in the thermal behavior of perhydrous bituminous coal during pyrolysis. J Therm Anal Calorim. 2015;119:2195–203.
6. Zhang Q, Li Q, Zhang L. Experimental and kinetic investigation of the pyrolysis, combustion, and gasification of deoiled asphalt. J Therm Anal Calorim. 2014;115:1929–38.
7. Ko KH, Aditya R, Veena S. Analysis of thermal degradation kinetics and carbon structure changes of co-pyrolysis between macadamia nut shell and PET using thermogravimetric analysis and ^{13}C solid state nuclear magnetic resonance. Energy Convers Manage. 2014;86:154–64.
8. Hu RZ, Gao SL, Zhao FQ. Thermal analysis kinetics. Beijin: Science Press; 2008.
9. Arenillas A, Rubiera F, Pis JJ. Simultaneous thermogravimetric–mass spectrometric study on the pyrolysis behavior of different rank coals. J Anal Appl Pyrolysis. 1999;50:31–46.
10. Deng J, Wang K, Zhang YN. Study on the kinetics and reactivity at the ignition temperature of Jurassic coal in North Shaanxi. J Therm Anal Calorim. 2014;118:417–23.
11. Herce C, Caprariis BD, Stendardo S. Comparison of global models of sub-bituminous coal devolatilization by means of thermogravimetric analysis. J Therm Anal Calorim. 2014;117:507–16.
12. Granada E, Eguía P, Comesaña JA. Devolatilization behaviour and pyrolysis kinetic modelling of Spanish biomass fuels. J Therm Anal Calorim. 2013;113:569–78.
13. Claudia U, Gordon AL, García X. Distribution of activation energy model applied to the rapid pyrolysis of coal blends. J Anal Appl Pyrolysis. 2004;71:465–83.
14. Achilias DS, Panayotidou E, Zuburtikudis I. Thermal degradation kinetics and isoconversional analysis of biodegradable poly (3-hydroxybutyrate)/organomodified montmorillonite nanocomposites. Thermochim Acta. 2011;51:58–66.
15. Iglesias MJ, Jiménez A, Del Río JC. Molecular characterisation of vitrinite in relation to natural hydrogen enrichment and depositional environment. Org Geochem. 2000;31:1258–99.
16. Xie KC. Coal Structure and reactivity. Beijing: Science Press; 2002.
17. Ibarra JV, Muńoz E, Moliner R. FTIR study of the evolution of lignite structure during the ligniteification process. Org Geochem. 1996;24:725–35.
18. Vassallo AM, Wilson MA, Edwards JH. ^{13}C n.m.r. Aromaticity balance on the products from flash pyrolysis of five Australian lignites. Fuel. 1987;66:622–6.
19. Yao ZZ, Han YX. Pyrolysis kinetics parameter of coal with different rank. Coal Chem Ind. 1994;67:340–2.
20. Su GQ, Cui CL, Lu HB. An analysis of the effect of the experimental condition on the performance of coal pyrolysis. Energy Technol. 2004;25:10–3.
21. Zhang N, Zeng FG, Jiang WP. Pyrolysis kinetics analysis of Chinese typical steam coals. J Taiyuan Univ Technol. 2005;36:449–52.
22. Liu SY, Tian YJ. Studies on pyrolysis and combustion of high volatile bituminous coals. J Fuel Chem Technol. 2002;30:412–4.
23. Zhu XD, Zhu ZB. Study on the effect of coal rank and heating rate on the pyrolysis. Coal Convers. 1999;22:432–47.
24. Xu YN. A study on coal pyrolysis reaction dynamics. J Eng Therm Energy. 1995;10:154–7.
25. Solomon PR, Serio M, Bassilakis R. Analysis of the Argonne Premium coal samples by thermogravimetric fourier transform infrared spectroscopy. Energy Fuels. 1990;4:319–33.
26. Burnham AK, Oh MS, Crowford RW. Pyrolysis of Argonne premium coals: activation energy distributions and related chemistry. Energy Fuels. 1989;3:42–55.
27. Zhao LH, Chu XJ, Xin GY. Research on pyrolysis characteristics and pyrolysis kinetics of coal. Coal Qual Technol. 2010;1:40–2.
28. Lu CW, Xi TG. Therm analysis-mass spectrometry. Shanghai: Shanghai Science and Technology Literature Press; 2002.
29. Yang JB, Zhang YW, Cai NS. A comparison of a single reaction mode with a distributed activation energy one based on coal pyrolysis kinetics. J Eng Therm Energy Power. 2010;25:301–5.
30. Zhou L, Luo T, Huang Q. Co-pyrolysis characteristics and kinetics of coal and plastic blends. Energy Convers Manage. 2009;3:705–10.
31. Xu Y, Zhang YF, Wang Y. Thermogravimetric study of the pyrolysis characteristics and kinetics of lignite. React Kinet Mech Catal. 2013;1:225–35.
32. Zhang C, Jiang X, Wei L. Energy convers. Manage. 2007;48:797–802.
33. Arenillas A, Rubiera F, Pevida C. A comparison of different methods for predicting coal devolatilisation kinetics. J Anal Appl Pyrolysis. 2001;58–59:685–701.
34. Puente G, Marban G, Fuente E. Modeling of volatile product evolution in coal pyrolysis: the role of aerial oxidation. J Anal Appl Pyrolysis. 1998;44:205–18.
35. Cai JQ, Wang YP, Zhou LM. Thermogravimetric analysis and kinetics of coal/plastic blends during co-pyrolysis in nitrogen atmosphere. Fuel Process Technol. 2008;89:21–7.